Power Electronics and Drives
Volume 9(44), 2024 DOI: 10.2478/pead-2024-0021

sciendo

Power Electronics and Drives

Constrained Series PI, PID and PIDA Controller Design Inspired by Ziegler–Nichols

Research paper

Mikulas Huba[1], Pavol Bistak[1], Jan Brieznik[1,*], Damir Vrancic[2]

[1]*Faculty of Electrical Engineering and Information Technology, Slovak University of Technology in Bratislava, Institute of Automotive Mechatronics, Bratislava, Slovakia*
[2]*Department of Systems and Control, Jožef Stefan Institute, Ljubljana, Slovenia*

Received: 30 December 2023; Accepted: 22 May 2024

Abstract: The present paper complements the results of several recent papers on higher-order (HO) controllers with automatic-reset. A modification of the two-step tuning of the constrained second-order derivative controllers based on integrator-plus-dead-time (IPDT) models is proposed. In the first step, the linear controller is designed using the multiple real dominant poles (MRDPs) method to avoid the slowdown of the closed-loop dynamics due to the presence of slow poles. In the second step, the smallest time constant of the numerator of the MRDP-optimal controller transfer function is selected as the automatic-reset time constant. The derived control method was tested on a thermal system for the filament disc dryer to demonstrate the deployment, tuning, use and impact of controllers with increasing derivative degree in practical applications. It is shown that the use of HO controllers is similar to the traditional hyper-reset controllers (i.e. series proportional-integral-derivative [PID] controllers) from the user's point of view. However, the advantages are faster transient responses while maintaining sufficiently smooth input and output shapes of the process with a minimum number of monotonic intervals. The overall design can be seen as a generalisation and discretisation of the Ziegler and Nichols graphical tuning method. One of the main new features is the consideration of a constrained control signal, as is typical for a pulse width modulated (PWM) actuator. Such actuators are often used in speed-controlled electric drives and in power electronics, among other applications.

Keywords: *performance portrait • multiple real dominant pole • constrained control • series PI • PID and PIDA controller*

1. Introduction

Series proportional-integral (PI) and proportional-integral-derivative (PID) controllers were already in use before the Second World War under their original designation as controllers with automatic reset and hyper-reset controllers. In some industries, pneumatic and analogue electronic automatic-reset devices are still an important part of control solutions. However, since the early days of linear theory in automatic control, the terms PI and PID controllers have been adopted, although the equivalence between the two types of controllers only applies to unlimited control. Another important difference is that although the automatic-reset-based controllers have not been based on explicit process models for decades, recently they have been interpreted as the first model-based solutions with reconstruction and compensation of input disturbances based on integral process models (Bistak et al., 2024; Huba et al., 2023a). Such an explicit and saturation invariant disturbance reconstruction does not exist in parallel PI and PID controllers without anti-windup protection. The integral term in PI and PID controllers is considered as a heuristic solution that guarantees a zero permanent deviation of the output from the setpoint value even in the presence of constant input and output disturbances.

As shown in several papers on this topic (such as Huba et al., 2023a), the mentioned types of controllers are not equivalent under constraints. The automatic-reset controllers and the hyper-reset controllers provide implicit protection against the windup effect, while the classical PI and PID controllers require additional internal feedback to protect them from the windup effect. In general, the tuning of the PID controller may require more computational

* *Email: jan.brieznik@stuba.sk*

effort than tuning a serial controller whose parameters can be directly derived from an integrating process model (Bistak et al., 2024).

Some misconceptions about controllers based on the auto-reset mechanism stem from the steps required to bring them to market, namely getting a patent protection by patent documents and writing a user manual. An example of the latter is Ziegler and Nichols' (1942) tuning rules, which do not explain the hidden nature of the controller or the process models, but the recommended settings were determined experimentally. Therefore, such rules cannot be directly applied in the search for the optimal tuning of a completely new generation of controllers based on digital technologies. Therefore, new interpretations of the Ziegler and Nichols method in terms of controller structure and process model were needed (Glattfelder and Schaufelberger, 2003) and produced in Takahashi et al. (1971). The mentioned work was already based on the local approximation of the process model by the integrator-plus-dead-time (IPDT) model and the three-term PID controller.

Even though the work by Ziegler and Nichols (1942) is the most frequently cited work on controller tuning, it cannot fulfil all practical requirements in its original version. Among the most frequently cited shortcomings are high overshoots and the oscillatory nature of transients (Buriakovskyi et al., 2022). In many mechatronic applications, e.g. in the speed control of electric drives, such transients are inadmissible. Therefore, a large number of other tuning rules were later developed based on a similar experiment of the process (see e.g Åström and Hägglund, 2004; Hägglund and Åström, 2002 and the references therein).

From the digital processing point of view, the identification of the inflection point in the process step response is numerically problematic. The solution proposed in Huba et al. (2021a) eliminates the calculation of the inflection point and introduces the analytical, model-based design of the series controllers with automatic-reset and hyper-reset. The mentioned work also illustrated the advantages of the automatic-reset and hyper-reset controllers, which have inherent anti-windup protection, compared to some additional 'anti-reset windup' blocks added to the ordinary parallel PID controllers.

Although the speed control system used in Huba et al. (2021a) has only a relatively low delay, a low-cost velocity sensor resulted in a relatively high measurement noise, which had to be attenuated by a low-pass filter. To 'combat' the reduced process speed due to the filter delay, a controller with higher-order (HO) derivatives (Bistak et al., 2023) is proposed. By using the same fourth-order filter and the IPDT approximation as in Huba et al. (2021a), the complexity of the optimal analytical calculation of the HO controller did not increase. Again, it was not necessary to take any anti-windup measures to obtain monotonic step responses (if such responses are needed). The motivation for using HO controllers came from replacing the dead time of the loop with the increasing number of its Taylor series expansion elements. The use of HO controllers is not new. So far, however, they have mainly been used in fractional-order PID controllers (Tepljakov et al., 2018; Thomson and Padula, 2022) (which can be realised by the Ostaloup approximation with HO integer-order controllers).

Thus, both the HO automatic-reset based and the PID controllers offered an additional degree of freedom in controller tuning for time-delayed systems. The robustness of closed-loop responses due to unmodelled dynamics is a common denominator of the various existing contributions on this topic (Arulvadivu et al., 2022; Boskovic et al., 2020; Ferrari and Visioli, 2022; Jung and Dorf, 1996a,b; Kumar et al., 2023; Kumar and Hote, 2021a,b,c; Oladipo et al., 2021; Sahib, 2015; Ukakimaparn et al., 2009; Veinovic et al., 2023; Visioli and Sánchez-Moreno, 2022; Zandavi et al., 2022). Some of the papers use the acronym from the proportional-integral-derivative-acceleration (PIDA) and the others from the second-order derivatives (PIDD2, or PIDD2). Another common feature of numerous publications is the use of numerical optimisation to find the controller setting. Since the pioneering work (Astrom et al., 1998), the range of different numerical optimisation and artificial intelligence methods has grown tremendously. Let us illustrate this growth with some recent approaches for optimising PIDA controllers:

- For the automatic voltage regulator (AVR) of a synchronous generator (Sahib, 2015), minimised the integral of time-weighted absolute error (ITAE) using particle swarm optimisation.
- The optimal design of a HO non-linear time-delayed system using a modified butterfly optimisation algorithm was addressed in Arulvadivu et al. (2022).
- In Zandavi et al. (2022), the flight stability of a quadcopter in a noisy environment was investigated using a heuristic genetic filter design.
- In Kumar and Hote (2021c), the output voltage regulation of a DC-DC converter was calculated using a modified Gray–Wolf optimiser.

- In Oladipo et al. (2021), a combination of the flower-pollinated algorithm (FPA) and the pathfinder algorithm (PFA) was used to regulate combined load frequency and terminal voltage control systems.
- In Fawwaz et al. (2023), the AVR system was developed using whale optimisation, in Emiroglu and Gumus (2022), it was optimised using the coronavirus herd immunity optimiser and in Agwa et al. (2021), it was optimised using the Archimedes optimiser.
- In Calasan et al. (2021) and Micev et al. (2021), the parameters of the PIDA controller for the AVR system are determined by the equilibrium optimiser, which belongs to the class of metaheuristic algorithms, etc. A broader overview of classical and intelligent PID tuning methods is given, for example, in Bansal (2021), Borase et al. (2021) and Saxena and Biradar (2022).

Although there is obviously great interest in the HO-PID controller, it is noticeable that the HO structures have not been applied to the tried-and-tested, industrially used controllers with automatic-reset. The terminological barrier mentioned earlier may be the best explanation for why it happened. In this paper, we will discuss some other issues related to the commonly used interpretation of PID control and its design, and we will present a wide range of new possibilities based on the traditional methods.

One way to make HO-PID controllers usable in practice is to use a common filtering of all controller terms. Using the PIDA controller as an example, Bistak et al. (2024) show that at least three differential equations must be solved to ensure separate filters for the first and second derivatives. It is therefore easier to implement a common filter for which it is sufficient to solve two differential equations. By solving three equations, a more effective noise attenuation can be achieved. For controller tuning, the multiple real dominant pole (MRDP) method is already used in an early textbook on automatic control (Oldenbourg and Sartorius, 1944). The MRDP method optimises the time-delayed systems by requiring equally fast dominant time constants, thus excluding slow components that would reduce the speed of the transients. The advantage of the method is that it can also be applied directly to quasi-polynomials with a dead time element. It has been shown that the MRDP method provides excellent results (Bistak et al., 2024; Huba et al., 2023a) when designing controllers up to a considerably high derivative degree $m = 7$. However, even higher controller degrees can be designed without major limitations. More important, of course, is the proof that such an increase in controller order brings a significant advantage in practice. It is worth noting that the widely used fractional order (FO) PID control ultimately leads to a controller implementation with even HO approximations (Tepljakov et al., 2018).

Another line of research has focused on investigating the effect of simple process approximations inspired by the pioneering work of Ziegler and Nichols (1942) and Huba et al. (2021a) and extended by the recently published requirements for practice-oriented design (Bistak et al., 2024). These approximations allow for an interpretation based on open-loop step responses, which correspond to IPDT models and are referred to as ultra-local models. In numerous situations, one may intuitively expect that more complex models (such as the first-order time-delayed model (FOTD); Huba et al., 2021a) or the second-order unstable-zero models (Alfaro and Vilanova, 2013) should provide more accurate results. However, numerous experiments have confirmed that the controller design with more complex models is not always better than the IPDT-based design. This raises the question of the extent to which the use of more complex models is justified when the actual structure of the controller used originates from simpler (e.g. IPDT) models. IPDT models simplify the process identification and controller design stages. They also make it possible to neglect the internal process feedback loops, which depend significantly on the external load. Such simplification is welcome, especially for higher derivative degrees m. In Huba et al. (2023a), the IPDT model was used for the automatic-reset based controllers with $m \in [0,5]$. However, the used upper bound for m was chosen only with respect to the space limitations of the article and, as shown in Bistak et al. (2024), it was already increased to $m = 7$, which may not be the final value. The increase in robustness of controllers based on simpler ultra-local IPDT models compared to more complex local FOTD can be generalised even further. The design of controllers based on IPDT models implies a more complex process where it seems necessary to use the HO models. In this work, we demonstrate this using the control of a filament dryer for FDM 3D printers (Briežnik et al., 2023). Similar to the HO-PID controllers, the HO derivatives can accelerate the transients in the closed loop. Increasing the speed requires considering the output limitations of the controller and using explicit integration and anti-windup circuitry. The conditioning technique (Hanus et al., 1987; Huba et al., 2021b) provides a successful anti-windup protection, at least for the realisation of 1-DOF controllers. In addition, implicit control (Hanus et al., 1987) has the same or similar form as the controller with automatic reset. However, in some cases where the overshoot of the limited input and output signals of the process should be prevented at all costs, this may not be the best control approach (Huba et al., 2021b). In the considered case of a filament dryer, the working temperature is set as high as possible, for example, just below the melting temperature of the medium, to shorten the drying process. In this case, transients with overshoot are therefore not permitted. For such control specifications, controllers with automatic reset (series controllers) with odd *m* prove to be more efficient (Bistak et al., 2023; Huba et al., 2023a). In these papers, the approach used in Huba et al. (2021a) was extended to all automatic-reset (series HO-PID) controllers tuned with the MRDP method. This fact can be considered as the most important aspect of the revival of the traditional solutions for automatic reset with positive feedback from the controller output. In order to take into account the limitations of the controller output, the numerator of the controller transfer function derived, using the MRDP method, must be factorised. The time constant of the automatic reset must be the smallest numerator time constant. However, the search for the smallest time constant becomes more complicated for even values of *m* if the numerator contains complex conjugate pole pairs. In such a case, the imaginary parts of the complex zeros can be neglected (Bistak et al., 2023; Huba et al., 2023a,b). The resulting double real zeros can still satisfy the absolute stability conditions based on the circle criterion for the controller with a saturation non-linearity (Huba et al., 2023a,b). Here, absolute stability is achieved for arbitrary initial states. To summarise, the new contribution of the paper can be specified as the development of new tuning rules for constrained series controllers with second-order derivatives with the illustrative example showing application of HO automatic-reset based controllers to filament dryer for FDM 3D printing.

The rest of the article is organised as follows. Section 2 deals with summarising the results regarding the structure and optimal tuning of the automatic-reset based controllers with $m \in [0,2]$ (i.e. series PI, PID and PIDA controllers) by the MRDP method. For constrained control, the MRDP tuning of series PIDA is modified by replacing the complex numerator transfer function zero of the controller with a double real one. The influence of such a double real approximation is analysed by searching for a single optional parameter based on the closed-loop performance measures. Section 3 shows and discusses the experimental results obtained by applying the derived PI, PID and PIDA controllers in the control of a filament dryer for FDM 3D printers (Briežnik et al., 2023). The conclusions summarise the obtained results of the work from a broader perspective.

2. Optimal PI, PID and PIDA Controller Tuning for IPDT Models by the MRDP Method

A process with the output *y*(*t*) and the input *u*(*t*) is described as follows

$$S(s)=\frac{Y(s)}{U(s)}=S_0(s)e^{-T_{dp}s};\; S_0(s)=\frac{K_{sp}}{s} \tag{1}$$

This is a two-parameter model specified by K_{sp} and T_{dp}. In some situations corresponding to the 'nominal process', it will be easier to omit the index *p* and work with the system parameters K_s and T_d. The input of the controller is called an error.

$$E(s)=W(s)-Y(s) \tag{2}$$

It represents the difference between the reference setpoint $W(s)$ and the process output $Y(s)$. The model-based approach, formulated for an integral process model described by a differential equation $y'=K_s.u+d_i.\, y'=dy/dt$, reconstructs the value of a constant input disturbance d_{irec} as the difference between the estimated input of the process $u_a=y'/K_s$ and the output of the (constrained) controller u_r as $d_{irec}=y'/K_s-u_r$. The calculation of the reconstructed disturbance must be supplemented by a low-pass filter $F_R(s)$ with a time constant T_i (see e.g. Bistak et al., 2023; Huba et al., 2023a).

$$F_R(s)=\frac{1}{1+T_i s} \tag{3}$$

By choosing the time constant T_i to be significantly larger than the time constant of the closed loop transients, the first term y'/K_s can be neglected in the vicinity of steady states and the disturbance value can simply be calculated as $d_{irec} = -u_r$. Since d_i must be compensated by $-d_{irec}$, it is possible to set up a positive feedback loop that modifies the output of the stabilising controller R_P in combination with a low-pass filter Q_n (Bistak et al., 2023; Huba et al., 2023a,b) (explained later) (see Figure 1). In the presence of a time delay T_d in Eq. (1), this can be replaced by developing to a Taylor series with a gradually increasing number of members, which increases the order of the equivalent transfer function *S* and thus also the order of the required control vector, which is suggested, for example, by using the state-space approach. Its special case is the phase vector, which is formed from the output and its derivatives. In this article, we will gradually increase the order of the stabilising controller, starting with a proportional controller K_p up to a proportional-derivative-accelerative (PDA), with the gains K_p, K_d, K_a, which is described as follows

$$R_p(s) = K_p + K_d s + K_a s^2 \tag{4}$$

The resulting structure with the positive feedback can be described as a series-proportional-integral-derivative-accelerative (PIDA) controller. It should be emphasised once again that the time constant T_i of the automatic reset can only be defined as an integration time constant in the zone of proportional control if it applies to the transfer function of the closed control loop (Eq. (5)).

In the case of a nominal plant (Eq. (1)) specified with K_s and T_d, the PIDA controller

$$R(s) = \frac{U(s)}{E(s)} = \frac{R(s)}{1 - F_R(s)} = \frac{\left(K_p + K_d s + K_a s^2\right)\left(1 + T_i s\right)}{T_i s} \tag{5}$$

results in

$$F_c(s) = \frac{Y(s)}{W(s)} = \frac{R(s)S(s)}{1 + R(s)S(s)} = \frac{K_s\left(K_p + K_d s + K_a s^2\right)\left(1 + T_i s\right)}{s^2 T_i e^{T_d s} + K_s\left(K_a s^2 + K_d s + K_p\right)\left(1 + T_i s\right)} \tag{6}$$

From a formal point of view, we obtain the relationships describing the PI controller by setting $K_d = K_a = 0$. In the case of a PID controller, $K_a = 0$ must be taken into account. Once again, it should be noted that the positive feedback from the output of the constrained controller gives the series PIDA transfer function (Eq. (5)) only for the unconstrained output of the controller, i.e. in the proportional zone of the control, if the always present limits are not exceeded:

$$u \in \left[U_{min}, U_{max}\right] \tag{7}$$

However, the equivalence of the automatic-reset-based controllers with the parallel PI, PID and PIDA controllers with the same transfer function in the vicinity of the steady states does not mean that their general equivalence applies to any initial states. In the case of constrained control, the positive feedback of the automatic reset cannot

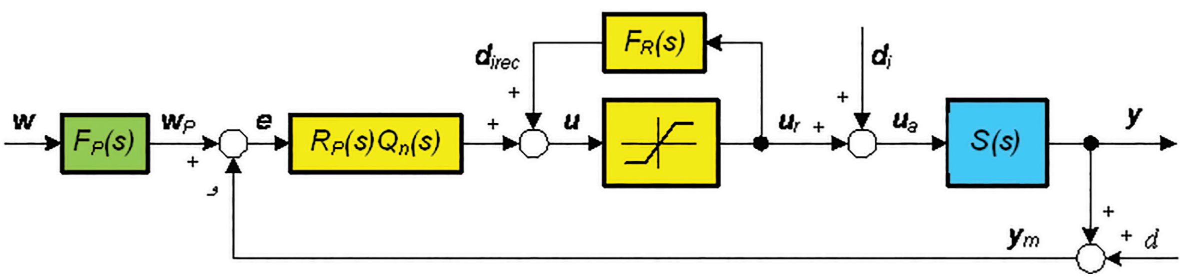

Figure 1. 2DoF HO automatic-reset (series HO PID) controller using a HO stabilising PD^m controller $R_p(s)$ (Eq. (4)) with a low-pass implementation filter $Q_n(s)$ (Eq. (9)), setpoint *w*, input disturbance d_i, output *y*, measurement noise δ, measured output $y_m(t)$, the automatic-reset in form of a positive feedback filter $F_r(s)$ (Eq. (3)) with the time constant T_i for reconstruction of an input disturbance d_{irec}, saturation non-linearity accomplishing Eqs (7) and (8) and prefilter $F_p(s)$ (Eq. (20)). HO, higher-order; PID, proportional-integral-derivative.

change the output of the stabilising controller with a signal that exceeds the limits of Eq. (7). In contrast, the I-action value of parallel controllers can still grow indefinitely, which further significantly changes the dynamics of the system after reaching a narrower range of desired states. This then affects the necessary changes to both solutions. The excessive integration (windup) of integrating controllers that occurs under constrained control can be reduced by various anti-windup schemes (Huba et al., 2021b, 2023b). On the other hand, to ensure the correct operation of automatic-reset controllers based on the feedback of the saturation non-linearity output:

$$u(t) = sat\{u_L\} = \begin{cases} U_{max}; & u > U_{max} \\ u_L; & U_{min} \le u_L \le U_{max} \\ U_{min} & u < U_{min} \end{cases} \tag{8}$$

which is added to the P, PD or PDA output u_L., only a suitable tuning of the controller parameters, including the time constant T_i, is required.

2.1. Design of controller filters

The implementation of derived PD and PDA controllers (Eq. (4)) requires the design of low-pass filters that guarantee at least a proper transfer function. The minimum number of unknown filter parameters corresponds to a single binomial filter $Q_n(s)$ with a sufficiently high relative degree *n* (Bistak et al., 2023)

$$Q_n(s) = \frac{Y_f(s)}{Y(s)} = \frac{1}{(T_f s + 1)^n} = \frac{1}{P_n(s)} \tag{9}$$

The equivalent filter delay can already be taken into account when approximating the process with the IPDT or FOTD model, as in Huba et al. (2021a) and Bistak et al. (2023), or the filter delay can be approximated by a chosen delay equivalence (Huba et al., 2023b), where the process delay T_{dp} is extended into the 'total' loop dead time by an 'equivalent' filter delay T_e

$$T_d = T_{dp} + T_e \tag{10}$$

This is much simpler than solving the filter parameters separately for the derivative and for the acceleration component of the controller (Ferrari and Visioli, 2022; Kumar and Hote, 2021c; Visioli and Sánchez-Moreno, 2022). As the derivative degree increases, this unnecessarily increases the number of filter time constants used, and the inclusion of different delays in particular controller channels complicates the analytical design (Bistak et al., 2024).

T_e in Eq. (10) can be calculated by various equivalences (Huba et al., 2023b), e.g. according to

$$T_e = nNT_f;\; N \in [0.5, 1] \tag{11}$$

where the weighting parameter N is specified by values from $N = 0.5$ (equivalence based on the 'half rule') to $N = 1$ (equivalence based on the 'average residence time').

2.2. Optimal MRDP controller setting

Since the speed of the transients depends predominantly on the slowest mode of the solution, slow modes of control can be eliminated by the MRDP method. Such a design also takes into account the fastest components of the solution, which are critical from the point of view of overshoot and oscillations (solution stability). The advantage of the real multiple pole condition is its simple determination. For a controller of derivative degree m, the dominant pole multiplicity depends on the number of unknown parameters of the controller $m+2$. Another unknown is the position of the pole itself, i.e. there are a total of $m+3$ unknown parameters. For the most complex PIDA controller, a total of five unknowns must be determined. In order to calculate the corresponding dominant pole, the equations

$$\left[\frac{d^i}{ds^i} A(s)\right]_{s=s_0} = 0; i = 0,1,\ldots,m+2 \tag{12}$$

must be fulfilled, where

$$A(s)=s^2T_ie^{T_ds}+\left(K_sK_as^2+K_sK_ds+K_sK_p\right)(1+T_is) \tag{13}$$

is the characteristic quasi-polynomial of Eq. (6). In general, the location of the optimal MRDP pole $s_0=-1/T_0$ (Arulvadivu et al., 2022) is

$$s_0=\left(\sqrt{m+2}-(m+2)\right)/T_d \tag{14}$$

For series PI controller with $m=K_a=K_d=0$, the following controller parameters are obtained (see e.g Huba et al., 2021a).

$$s_0=\left(\sqrt{2}-2\right)/T_d\approx-0.5858/T_d;K_p=\frac{2\left(\sqrt{2}-1\right)e^{\sqrt{2}-2}}{K_sT_d}\approx\frac{0.4612}{K_sT_d};T_i=\frac{\left(\sqrt{2}-1\right)T_d}{10\sqrt{2}-14}\approx5.8284T_d \tag{15}$$

For PID controllers with $m=1$; $K_a=0$, it is possible to obtain a set of MRDP controller parameters with the smallest possible T_i for the stabilising controller $R(s)=K_p+K_ds=K_p(1+T_Ds)$ in Figure 1 (see e.g. Huba et al., 2021a,b) as

$$s_0=\left(\sqrt{3}-3\right)/T_d\approx-1.2679/T_d;K_p\approx\frac{0.0598}{K_sT_d};T_i\approx0.2846T_d;T_D\approx3.4475T_d;K_d=K_pT_D\approx\frac{0.2062}{K_s} \tag{16}$$

Compared to the PI controller, the value of T_i is significantly smaller, which has an impact on the disturbance reconstruction and compensation. In addition to the reduced value of K_p, the strengthening of the derivative component K_d also contributes to stability.

In the case of the most complex PIDA controllers with $m=2$, the solution of $\mathrm{d}^4A(s)/\mathrm{d}s^4=0$ corresponding to the dominant pole s_0 (or the equivalent time constant T_0) results in

$$s_0=-2/T_d;T_0=-1/s_0=T_d/2 \tag{17}$$

The remaining Eq. (12) then results in Huba et al. (2023b)

$$K_p=\frac{0.9323}{K_sT_d};K_d=\frac{0.3885}{K_s};K_a=\frac{0.0451}{T_dK_s};T_i=2.5832T_d \tag{18}$$

The corresponding time constants of the controller's numerator are

$$T_D=K_d/K_p=0.4168T_d;\ T_A^2=K_a/K_p=0.0484T_d^2 \tag{19}$$

is important for tuning the controller with two degrees of freedom (2DoF). Since the PI, PID and PIDA controllers with one degree of freedom (1DoF) result in setpoint step responses with a high overshoot, 2DoF controllers can be proposed by introducing a prefilter that removes the zeros from the $F_c(s)$ (Eq. (6))

$$F_p(s)=\frac{b_3s^3+b_2s^2+b_1s+1}{\left(T_A^2s^2+T_Ds+1\right)(T_is+1)} \tag{20}$$

For PID, $T_A^2=0$, for PI $T_A^2=T_D=0$ and the numerator degree must be reduced accordingly. For constrained control, the simplest and most robust choice is to set

$$b_3=0;\ b_2=0;\ b_1=0 \tag{21}$$

in Eq. (20). As in Viteckova and Vitecek (2016), an acceleration of the setpoint step responses is possible by designing the $F_p(s)$ numerator, which can be used to cancel at least one time constant in the closed control loop T_0 (Eq. (17))

$$b_3 = 0;\ b_2 = 0;\ b_1 = T_o = T_d/2 \tag{22}$$

An overview of the dependence of the optimal setting on the degree of derivative *m* used is best obtained by using dimensionless parameters in Table 1. It shows that the dominant time constant of the circuit τ_0 becomes shorter as m increases, while even for $m=0$ and $m=2$, it is significantly smaller than the automatic-reset time constant τ_i. With unconstrained control, the MRDP PI, PID and PIDA controllers provide ideal shapes of responses characterised by a minimum number of monotonic segments at the process input and output after both setpoint and input disturbance steps. However, with limited control, MRDP-optimal controllers can lead to the overshoot of output and input. Since such imperfections occur in parallel PI, PID and PIDA controllers even when using the anti-windup modifications based on the conditioning technique (Huba et al., 2021b), the first question was therefore whether it is at all possible to avoid them with a modified controller setting. Basically, this effort is equivalent to achieving absolute stability of the given constrained system (Follinger, 1993; Glattfelder and Schaufelberger, 2003; Haddad and Chellaboina, 2011; Khalil, 1996; Lima, 2021; Popov, 1961). When using a PI controller, there is no possibility to fulfil the condition of absolute stability. In the case of PID control, this corresponds to the parameters Eq. ((16)).

2.3. Constrained series PIDA controller tuning

The optimal setting of the constrained series PIDA controller was first optimised numerically using the performance portrait method (PPM) (Huba et al., 2023c). It was derived by mapping the closed-loop performance for different controller settings and selecting the best controller parameters as those that give the minimum integral of absolute error (IAE) corresponding to the performance specified by the monotonicity-based performance measures of the disturbance responses

$$TV_1(y_d) \le \epsilon_{yd}; TV_1(u_d) \le \epsilon_{ud}; \epsilon_{yd} = \epsilon_{ud} = 0.001 \tag{23}$$

with

$$\begin{aligned} TV_1(y) &= \sum_i |y_{i+1} - y_i| - |2y_m - y_\infty - y_0|;\ y_m \notin (y_0, y_\infty) \\ TV_1(u) &= \sum_i |u_{i+1} - u_i| - |2u_m - u_\infty - u_0|;\ u_m \notin (u_0, u_\infty) \end{aligned} \tag{24}$$

Thereby, y_{max} and u_{max} represent the extreme points separating two monotonic segments of one-pulse (1P) disturbance step responses at the input and output of the process (Huba et al., 2021a). Several series of experiments finally resulted in the optimal setting of the constrained PIDA controller

$$K_p = \frac{0.17}{K_s T_d};\ K_d = \frac{0.45}{K_s};\ K_a = \frac{0.1157 T_d}{K_s};\ T_i = 0.36 T_d;\ T_D = K_d/K_p = 2.65 T_d;\ T_A^2 = K_a/K_p = 0.681 T_d^2 \tag{25}$$

Table 1. Dimensionless MRDP-optimal parameters of series PIDA controller, $\tau_0 = T_0/T_d, \kappa = K_p K_s T_d, \tau_i = T_i/T_d, \tau_D = T_D/T_d, \tau_A = T_A^2/T_d^2, m \in \{0,1,2\}$ corresponds to the used derivative degree.

	$m = 0$	$m = 1$	$m = 2$
τ_0	1.7071	0.7887	0.5000
κ	0.4612	0.059	0.9323
τ_i	5.8284	0.2846	2.5832
τ_D	0	3.4475	0.4168
τ_A	0	0	0.0484

MRDP, multiple real dominant pole.

With respect to the MRDP-PIDA parameters (Eq. (18)), K_p and T_i decreased and K_d and K_a increased. Increased values were also obtained for the time constants T_D and T_A^2. Figure 3 shows the transient responses corresponding to $T_{dp}=1$ and the filter $Q_4(s)$ tuned according to Eq. (11) ($n=4$ in Eq. (9)) with $N=1$, $T_e=0.8$ and $T_f=T_e/n=0.2$. With the aim of having 'tight control signal constraints', these were chosen separately for setpoint and disturbance responses and with a view to ensuring the possibility of reaching steady states. The simulation results obtained confirm that fast and smooth transients without overshoot are achieved at both the process input and output. Fast transients at the process input and output also lead to a faster reconstruction of the external input disturbances, which have to be compensated by automatic-reset.

In engineering, we are used to working with estimates of individual process parameters that have a certain final accuracy. However, from a practical point of view, it is always interesting to know how the steps of the dimensionless values $\Delta\kappa$, $\Delta\tau_D$, $\Delta\tau_A$ and $\Delta\tau_i$ used to check the optimal controller parameters in the four-dimensional parameter space $\kappa=K_pK_sT_d$, $\tau_D=T_D/T_d$, $\tau_A=T_A/T_d$ and $\tau_i=T_i/T_d$, which consists of 10^4 = 10,000 points, affect the achieved accuracy of the solution found (Eq. (25)). In general, the achieved accuracy of the optimal setting can be increased by decreasing the individual values Δ, which leads to an increase in the number of points considered for a given neighbourhood size. The other option is to 'zoom in' by reducing the neighbourhood by the previously found 'optimal' tuning while keeping a fixed number of evaluated points.

2.4. 'Suboptimal' 1D APR-PIDA controller tuning

Although the optimal tuning (Eq. (25)) was calculated by searching among the results of 10,000 simulations, the actual number of evaluated points, when including the experiments made to obtain some relevant neighbourhood of Eq. (25), was significantly higher. Therefore, it is of great practical importance to search for some suboptimal tuning methods that allow experimentally finding a near-optimal controller with a significantly lower number of evaluated points (Huba et al., 2023b,c). The aim of such modifications was to generalise the series PID controller (Huba et al., 2021a), where the time constant of the automatic reset is determined by factorising the numerator of the MRDP controller and choosing T_i as the smallest time constant. Such an approach does not affect the excellent performance of the linear MRDP controllers, but allows to modify the dynamics of the constrained non-linear system with saturation. However, in the case of the PIDA controller, the factorisation is not fully applicable due to the complex conjugate zero of the numerator of the MRDP controller Eq. (5) $T_A^2s^2+T_Ds+1=0.0484s^2T_d^2+0.4168T_ds+1$, expressed as

$$s_{1,2}=(-4.3058\pm1.4565j)/T_d \tag{26}$$

The single real zero in the numerator results in a too long time constant for the automatic reset $T_i=2.5832T_d$, which leads to slow transients with overshoot at saturation (Astrom and Hagglund, 1995, 2006; Kothare et al., 1994). By neglecting the imaginary part in Eq. (26), it was possible to obtain a double real pole $s_{1,2}=-4.3058/T_d$, which corresponds to the much shorter double real numerator time constant $T_2\ll T_i=2.5832T_d$

$$T_2=T_d/4.3058\approx0.232T_d \tag{27}$$

Such a modified nomination for T_i makes it possible to change the dynamics of the automatic reset at the transition from the saturation limit to the steady state and thus prevent overshoot. Since the transfer function of the controller remains almost the same, the dynamics of the linear system do not change significantly. With the new choice $\bar{T}_i=T_2$, the modified equations of the controller become

$$K_P\frac{(1+T_2s)^2(1+T_is)}{T_is}=\bar{K}_P\frac{(1+T_2s)(1+T_is)(1+T_2s)}{T_2s}=\bar{K}_P\frac{(1+\bar{T}_Ds+\bar{T}_A^2s^2)(1+\bar{T}_is)}{\bar{T}_is} \tag{28}$$

which can be rearranged to

$$\bar{K}_p=K_p\frac{T_2}{T_i};\bar{T}_i=T_2;\bar{T}_D=T_i+T_2;\bar{K}_d=\bar{K}_{p\bar{T}_D};\bar{T}_A^2=T_iT_2;K_a=\bar{K}_p\bar{T}_A^2. \tag{29}$$

If we start the recalculation with the MRDP controller (Eq. (18)), we obtain the PIDA$_1$ controller

$$\overline{K}_p = \frac{0.9323 \cdot 0.232}{2.5832 K_s T_d} = \frac{0.0837}{K_s T_d}; \overline{T}_i = 0.2320 T_d; \overline{T}_D = 2.8152 T_d; \overline{K}_d = \frac{0.236}{K_s}; \overline{T}_A^2 = 0.5993 T_d^2; K_a = \frac{0.0502 T_d}{K_s} \quad (30)$$

The usefulness of the proposed tuning modification was confirmed by applying the circle criterion of absolute stability (Huba et al., 2023a,b,c). For the given non-linear circuit and saturation-type non-linearity, it was shown that the tuning based on Eqs (27)–(29) guarantees absolute stability for arbitrary initial states. However, from the point of view of practical applications, it was necessary to further pay attention to situations where the requirement $T_2 \neq 0.232 T_d$ is not exactly fulfilled. The given problem was clarified by simulating the circuit with the variable value $\tau_2 = T_2/T_d \in [0.2, 0.4], \Delta\tau_2 = 0.05$ (see Figure 2). In order to achieve a dominant influence of the control signal constraints, these were chosen as tight as possible. To enable a stable state to be achieved, it was necessary to select different constraints for setpoint and input disturbance steps.

The obtained performance measures in Figure 2 show that for setpoint step responses, the choice of $\tau_2 = 0.232$ represents the optimal value in terms of a near-zero deviation of the controller's output from its ideal 1P shape. If $\tau_2 < 0.2$ is further reduced, the measured shape deviations increase already relatively sharply. The shape deviations for $\tau_2 > 0.232$ increase slowly, the values of the IAEs also increase in a similar way. However, at the same time, the performance measures of the disturbance step responses improve, approximately up to the 50% of the higher value of τ_2, which corresponds to the simple replacement of the MRDP setting. For $\tau_2 = 1.5 * 0.232$, the set of settings corresponding to the PIDA$_2$ term can then be calculated

$$\overline{T}_i = 0.348 T_d; \overline{K}_p = \frac{0.126}{K_s T_d}; \overline{T}_D = 2.931 T_d; \overline{K}_d = \frac{0.368}{K_s}; \overline{T}_A^2 = 0.899 T_d^2; \overline{K}_a = \frac{0.113 T_d}{K_s} \quad (31)$$

Obviously, it works with higher gains than PIDA$_1$ (Eq. (30)), and in view of the better disturbance response, it is expected to be used for controlling processes with significant deviations of the dynamics from the IPDT approximation used.

It is also worth mentioning that PIDA$_1$ can perform better than PPM-PIDA. This is due to the fact that in PPM the optimal setting was determined only by evaluating disturbance step responses and that examining the possible settings of individual parameters with the finite Δ values yields only finite accuracy in the search for the optimum.

The responses in Figure 3 show the comparison of MRDP-PIDA, PPM-PIDA, PIDA$_1$ and PIDA$_2$ controllers. The reconstructed disturbance was also recorded to illustrate the long overlooked function of automatic-reset as the simplest disturbance observer. The responses confirm that when MRDP tuning is used, overshoots of the output and input of the process occur as a result of control constraints. The use of PPM-PIDA led to a significant improvement in the transients achieved. However, its calculation is significantly more demanding than the changes

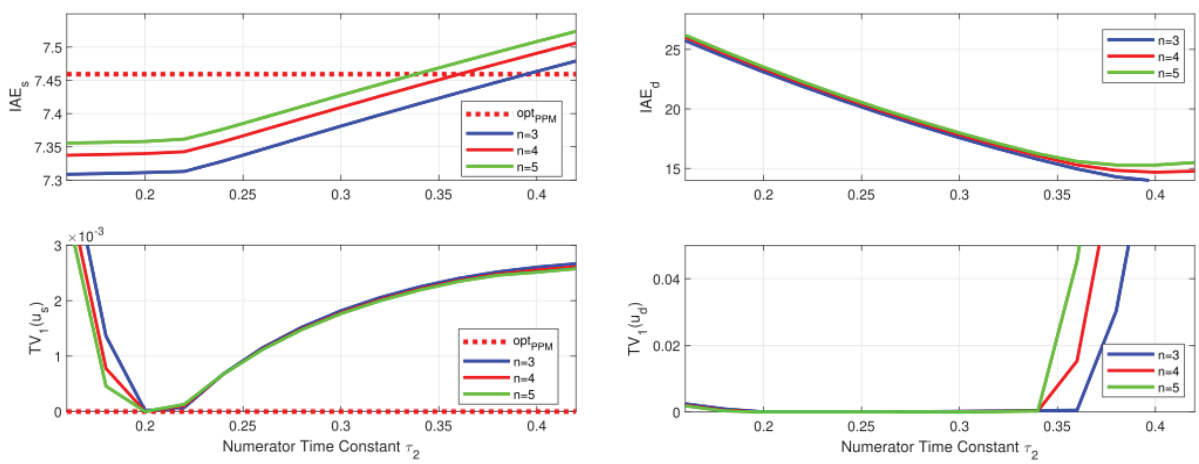

Figure 2. Impact of numerator time constant τ_2 selection of PIDA$_1$ control for different low-pass filter degrees n ($\tau_2 \in [0.16, 0.42], \Delta\tau_2 = 0.02$) on performance of setpoint responses ($U_{max} = 0.1, U_{min} = -0.1$, left) and disturbance responses ($U_{max} = 0.1, U_{min} = -1.1$, right). IAE, integral of absolute error.

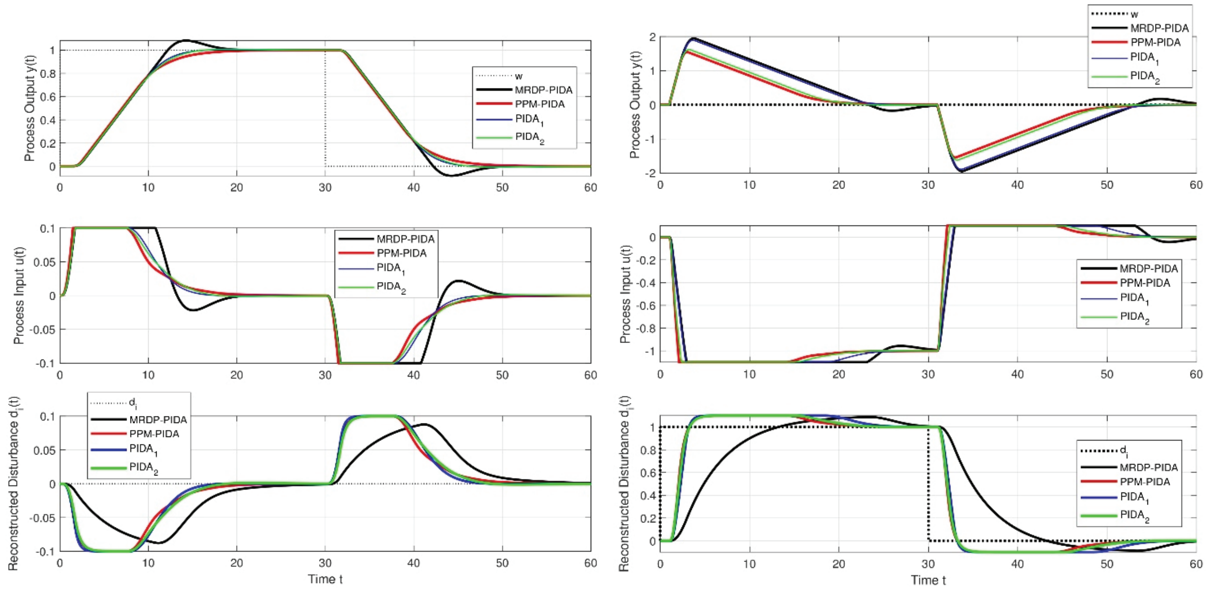

Figure 3. Setpoint and input disturbance step responses of constrained series MRDP-, PPM-, $PIDA_1$ and $PIDA_2$ controllers with $U_{max} = 0.1, U_{min} = -0.1$; for the unit setpoint steps and $U_{max} = 0.1, U_{min} = -1.1$ for the unit input disturbance steps, filter $Q_4(s)$ with $T_e = 0.8$; $T_f = T_e/n = 0.2$, $K_s = 1$, $T_{dp} = 1$ and the sampling period $T_s = 0.001$. MRDP, multiple real dominant pole; PPM, performance portrait method.

made in the calculation of the $PIDA_1$ and $PIDA_2$ controllers. While $PIDA_1$ provides slightly better transients for the setpoint responses, $PIDA_2$ is significantly better for the disturbance responses.

3. Application to Filament Dryer for FDM 3D Printing

The control objectives, basic design features and achieved properties of the filament dryer for FDM 3D printing (Figure 4) were recently published in Briežnik et al. (2023). In the temperature control required to dry the material as quickly as possible, it is necessary to ensure that the temperature values that may cause damage to the structure and the dried material itself are not exceeded. To be able to work with the new material as quickly as possible, the proposed temperature control system should of course work as close as possible to the structural limits of the system. At the same time, the system should be sufficiently robust so that it does not depend on the differences resulting from the different temperature properties of the actual material used. Next, we show the closed-loop results of a series PI, PID and PIDA controllers tuned according to a step response identification experiment inspired by Ziegler and Nichols (1942).

3.1. Step response-based process approximation

Ziegler and Nichols' original method was based on determining the tangent that passes through the inflection point of the measured process step response curve. Such a tangent can be used to determine the parameters of the IPDT and the first-order time-delayed process model (FOTD). Because finding a tangent line is a mathematically ill-conditioned problem, we have replaced it with a simple approximation using the least squares method (Huba et al., 2021a). The identification method finds the solution with the largest dead time value or model gain among different possible models. In the case of the IPDT approximation, the selection of the largest gain or dead time can be justified by a more detailed analysis of the closed-loop robust stability. Similarly to Huba et al. (2023b) or Huba et al. (2021a), the noise filter at the input of the controller was assigned to the controlled process, so it was not necessary to consider it as an additional equivalent delay T_e in Eq. (10). The disadvantage of such a method is that we cannot simply change the filter parameters without redrawing the new filtered response. However, the approach proposed here is simpler. The IPDT model of the system, including the fourth-order filter with $T_f = 50\,\mathrm{s}$ (see Figure 5), gives the parameters

$$K_s = 8.31 \cdot 10^{-4}\ \mathrm{K} \cdot (\mathrm{Vs})^{-1}; T_d = 74.5\,\mathrm{s} \tag{32}$$

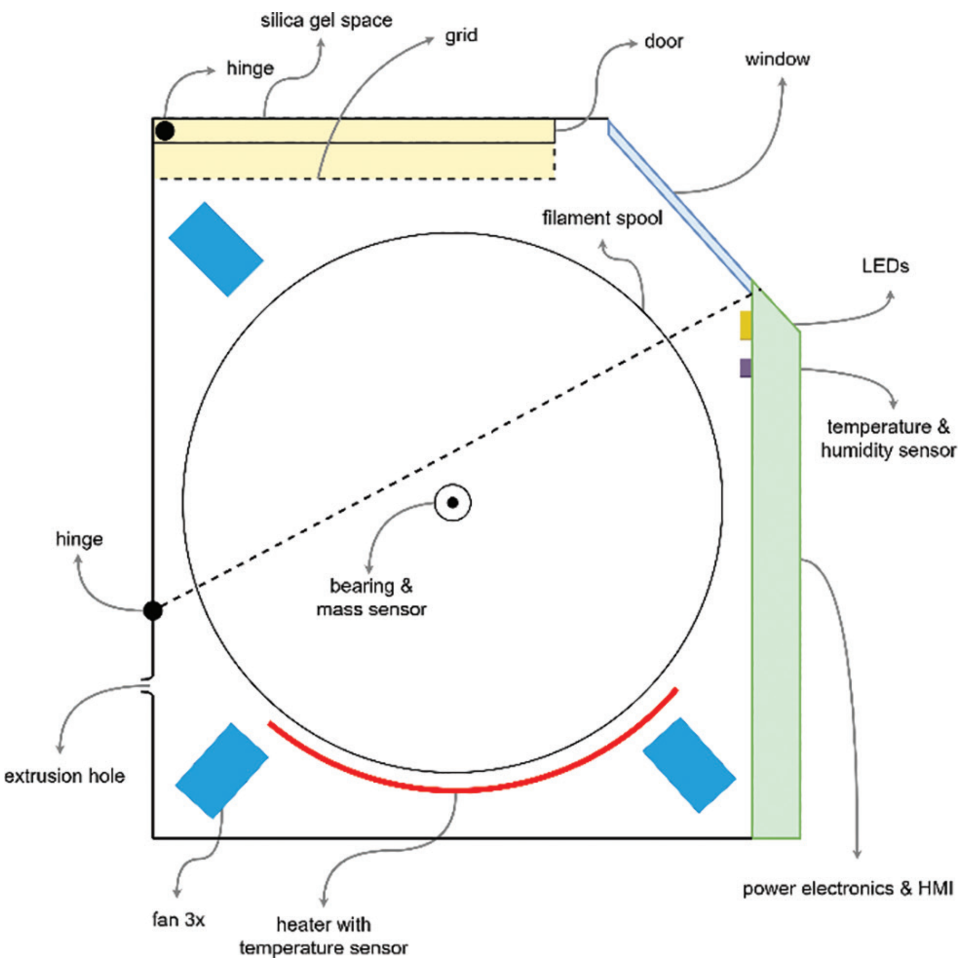

Figure 4. Filament dryer schema.

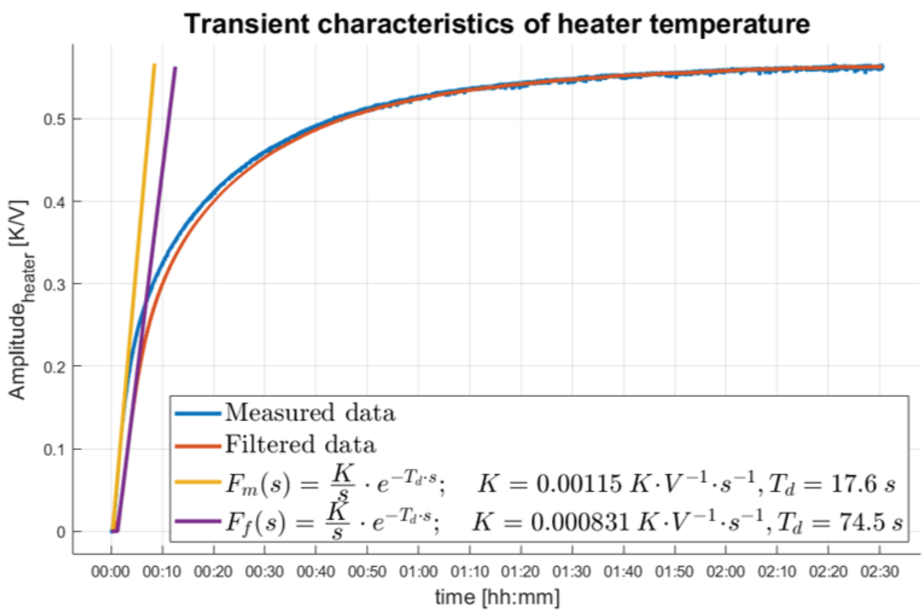

Figure 5. Measured step response of the system and its filtration achieved by application of the 4th order filter $Q_4(s)$ (Eq. (9)) with $T_f = 50$ s.

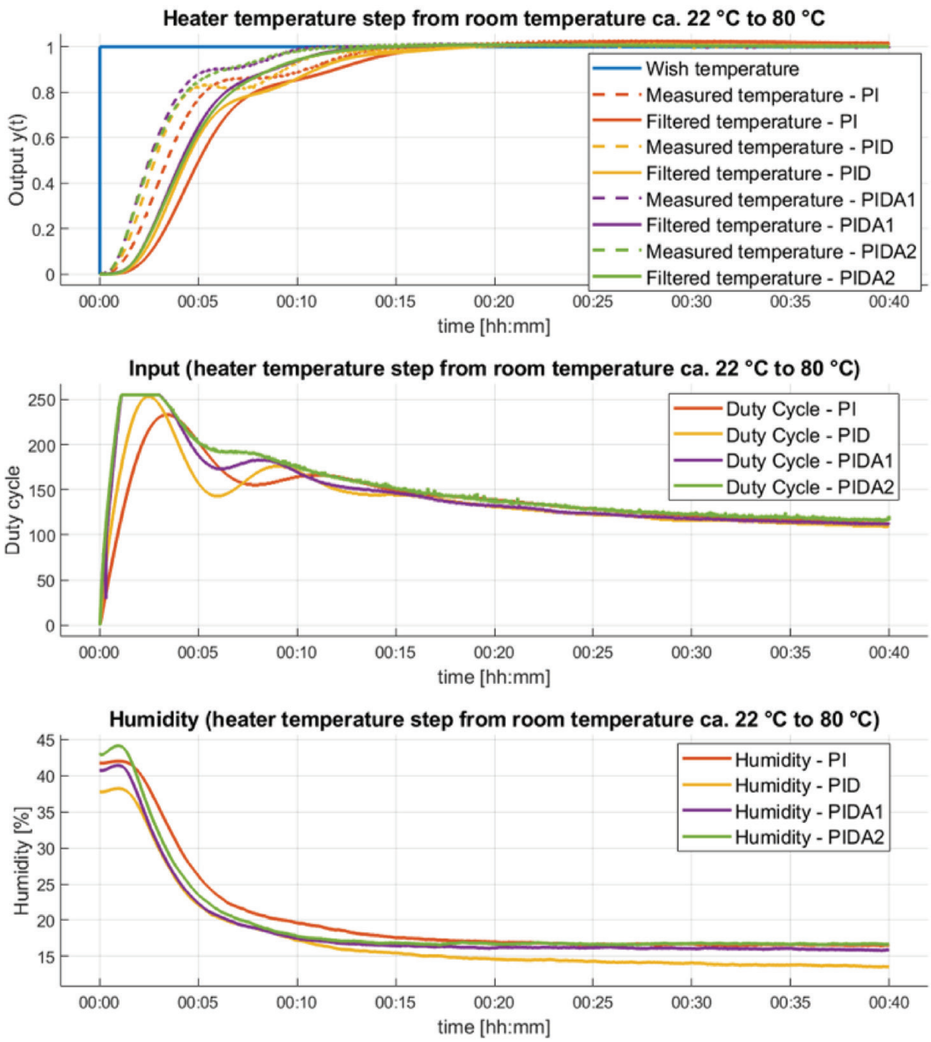

Figure 6. Closed loop step response at the input and output of the system and its filtration achieved by application of the 4th order filter $Q_4(s)$ (Eq. (9)) with T_f = 50 s and PI (Eq. (15)), PID (Eq. (16)) and PIDA (Eq. (29)) controllers. PI, proportional-integral; PID, proportional-integral-derivative.

As far as the unfiltered signal is concerned, the applied filter does not lead to significantly slower transients.

3.2. Closed loop step responses

The heating element is supplied by a transistor, which is switched by pulse width modulation (PWM) generated by the Arduino UNO microcontroller. The maximum supply voltage is 24 V. The sampling period was set to 0.5 s. The duty cycle in Figure 6 below corresponds to the limited pulse width of 0–255. The measured step responses of the closed loop in Figure 6 show that the temperature of the heater does not exceed the reference value of 80°C, and by increasing the derivatives of the controller order, the transients accelerate. Using an MRDP PID controller with numerator factorisation of the calculated transfer function by selecting the smallest numerator time constant as T_i confirms the improved closed loop dynamics. The factorisation of the transfer function of the MRDP PIDA controller has a similar effect and the step response of the output remains almost monotonic despite the limited input.

4. Discussion

Although the signal measured during identification has a measurement noise, the control signal of the PIDA controller is also sufficiently smooth and efficient. It is also clear to see that increasing m (the number of derivative terms) clearly contributes to the acceleration of the transients. Obviously, with the given filter $Q_4(s)$ and the IPDT model (Eq. (32)), it would be possible to further increase the range of controller derivatives used (see e.g Huba et al., 2023a) and thus increase its robustness and the speed of the transients.

5. Conclusions

The presented work is part of a broader research in the field of generalisation of industrial automatic reset and hyper-reset controllers when using HO derivatives and tuning controllers by the MRDP method. The results obtained show that despite the invention of the automatic-reset and hyper-reset controllers and tuning methods (by Ziegler and Nichols) in the 1940s, the advantages of the controller structure have not been sufficiently recognised by the scientific community. The analysis of the controllers mentioned here enables further generalisations and implementation in practice owing to the increase in the robustness of the controllers. The precise design of automatic-reset and hyper-reset controllers inspired by the Ziegler and Nichols tuning method can overcome their traditional limitations, which is particularly welcome in the field of mechatronics. The given analysis is particularly important when trying to transfer the historical hardware solutions into discrete programmable devices, embedded systems, sensors and actuators. The proposed solutions were tested in practice, where they showed high robustness, which can also significantly simplify process identification. Another important advantage is simplified filtering with implicit constrained control, which is crucial for successful PWM control.

Acknowledgment

This research was supported in part by the following grants: call for PhD students and young researchers of Slovak University of Technology in Bratislava to start a research career grant 23-11-57-21. Call for PhD students and young researchers was supported by call 09I03-03-V05, financed by RRP SR; Grant No. 1/0107/22 financed by the Scientific Grant Agency of the Ministry of Education, Research, Development and Youth of the Slovak Republic; Grant No. APVV-21-0125 financed by the Slovak Research and Development Agency; Slovenian Research and Innovation Agency – Research Program P2-0001, by Clean Hydrogen Partnership (EU Horizon 2020) under Grant Agreement No. 101007175 (project REACTT).

References

Agwa, A., Elsayed, S. and Ahmed, M. (2021). Design of Optimal Controllers for Automatic Voltage Regulation Using Archimedes Optimizer. *Intelligent Automation and Soft Computing*, 31, pp. 799–815. doi: 10.32604/iasc.2022.019887.

Alfaro, V. M. and Vilanova, R. (2013). Robust Tuning of 2DoF Five-Parameter PID Controllers for Inverse Response Controlled Processes. *Journal of Process Control*, 23, pp. 453–462. doi: 10.1016/j.jprocont.2013.01.005.

Arulvadivu, J., Manoharan, S., Lal Raja Singh, R. and Giriprasad, S. (2022). Optimal Design of Proportional Integral Derivative Acceleration Controller for Higher-order Nonlinear Time Delay System using m-MBOA Technique. *International Journal of Numerical Modelling: Electronic Networks, Devices and Fields*, 35. doi: 10.1002/jnm.3016.

Astrom, K. J., Panagopoulos, H. and Hagglund, T. (1998). Design of PI Controllers based on Non-Convex Optimization. *Automatica*, 34, pp. 585–601. doi: 10.1016/S0005-1098(98)00011-9.

Astrom, K. J. and Hagglund, T. (1995). *PID Controllers: Theory, Design, and Tuning*, 2nd ed. NC: Instrument Society of America, Research Triangle Park.

Åström, K. J. and Hägglund, T. (2004). Revisiting the Ziegler-Nichols Step Response Method for PID Control. *Journal of Process Control*, 14, pp. 635–650. doi: 10.1016/j.jprocont.2004.01.002.

Astrom, K. J. and Hagglund, T. (2006). *Advanced PID Control*. NC: ISA, Research Triangle Park.

Bansal, S. (2021). Nature-Inspired Hybrid Multi-objective Optimization Algorithms in Search of Near-OGRs to Eliminate FWM Noise Signals in Optical WDM Systems and their Performance Comparison. *Journal of the Institution of Engineers (India) Series B*, 102. doi: 10.1007/s40031-021-00587-5.

Bistak, P., Huba, M., Chamraz, S. and Vrancic, D. (2023). IPDT Model-Based Ziegler-Nichols Tuning Generalized to Controllers with Higher-order Derivatives. *Sensors*, 23, p. 3787. doi: 10.3390/s23083787.

Bistak, P., Huba, M. and Vrancic, D. (2024). Practice-Oriented Controller Design for an Inverse-Response Process: Heuristic Optimization Versus Model-Based Approach. *Applied Sciences*, 14, p. 2890. doi: 10.3390/app14072890.

Borase, R., Maghade, D. K., Sondkar, S. Y. and Pawar, S. (2021). A Review of PID Control, Tuning Methods and Applications. *International Journal of Dynamics and Control*, 9, pp. 818–827. doi: 10.1007/s40435-020-00665-4.

Boskovic, M. C., Sekara, T. B. and Rapaic, M. R. (2020). Novel Tuning Rules for PIDC and PID Load Frequency Controllers Considering Robustness and Sensitivity to Measurement Noise. *International Journal of Electrical Power and Energy Systems*, 114, p. 105416. doi: 10.1016/j.ijepes.2019.105416.

Briežnik, J., Zakova, K. and Huba, M. (2023). Filament dryer for FDM 3D printing. In: *Proceedings of the 2023 International Conference on Electrical Drives and Power Electronics (EDPE)*, pp. 1–7. doi: 10.1109/EDPE58625.2023.10274024.

Buriakovskyi, S., Asmolova, L. V., Maslii, A. S., Maslii, A. S. and Obruch, I. (2022). Development and Study of a Microprocessor Automatic Control System for a Mono-Switch Tie Type with a Linear Inductive Electric Motor and a Discrete Speed Controller. *Electrical Engineering and Electromechanics*, pp. 3–9. doi: 10.20998/2074-272X.2022.5.01.

Calasan, M., Micev, M., Radulovic, M., Zobaa, A. F., Hasanien, H. M. and Abdel Aleem, S. H. E. (2021). Optimal PID Controllers for AVR System Considering Excitation Voltage Limitations Using Hybrid Equilibrium Optimizer. *Machines*, 9, p. 265. doi: 10.3390/machines9110265.

Emiroglu, S. and Gumus, T. (2022). Optimal Control of Automatic Voltage Regulator System with Coronavirus Herd Immunity Optimizer Algorithm-Based PID plus Second Order Derivative Controller. *Academic Platform Journal of Engineering and Smart Systems*, 10, pp. 174–183. doi: 10.21541/apjess.1149455.

Fawwaz, M. A., Bingi, K., Ibrahim, R., Devan, P. A. M. and Prusty, B. R. (2023). Design of PIDDα Controller for Robust Performance of Process Plants. *Algorithms*, 16, p. 437. doi: 10.3390/a16090437.

Ferrari, M. and Visioli, A. (2022). A Software Tool to Understand the Design of PIDA Controllers. *IFAC-PapersOnLine*, 55, pp. 249–254. 13th IFAC Symposium on Advances in Control Education ACE 2022. doi: 10.1016/j.ifacol.2022.09.287.

Follinger, O. (1993). *Nichtlineare Regelungen*. Munchen: R. Oldenbourg Verlag.

Glattfelder, A. and Schaufelberger, W. (2003). *Control Systems with Input and Output Constraints*. Berlin: Springer.

Haddad, W. M. and Chellaboina, V. (2011). *Nonlinear Dynamical Systems and Control: a Lyapunov-Based Approach*. Princeton University Press.

Hägglund, T. and Åström, K. J. (2002). Revisiting the Ziegler-Nichols Tuning Rules for PI Control. *Asian Journal of Control*, 4(4), pp. 364–380. doi: 10.1111/j.1934-6093.2002.tb00076.x.

Hanus, R., Kinnaert, M. and Henrotte, J. (1987). Conditioning Technique, a General Anti-Windup and Bumpless Transfer Method. *Automatica*, 23, pp. 729–739. doi: 10.1016/0005-1098(87)90029-X.

Huba, M., Bistak, P. and Vrancic, D. (2023a). Series PID Control with Higher-order Derivatives for Processes Approximated by IPDT Models. *IEEE Transactions on Automation Science and Engineering*, pp. 1–13. doi: 10.1109/TASE.2023.3296201.

Huba, M., Bistak, P. and Vrancic, D. (2023b). Parametrization and Optimal Tuning of Constrained Series PIDA Controller for IPDT Models. *Mathematics*, 11(20), p. 4229. doi: 10.3390/math11204229.

Huba, M., Bistak, P. and Vrancic, D. (2023c). Series PIDA Controller Design for IPDT Processes. *Applied Sciences*, 13, p. 2040. doi: 10.3390/app13042040.

Huba, M., Chamraz, S., Bistak, P. and Vrancic, D. (2021a). Making the PI and PID Controller Tuning Inspired by Ziegler and Nichols Precise and Reliable. *Sensors*, 18, p. 6157. doi: 10.3390/s21186157.

Huba, M., Vrancic, D. and Bistak, P. (2021b). PID Control with Higher Order Derivative Degrees for IPDT Plant Models. *IEEE Access*, 9, pp. 2478–2495. doi: 10.1109/ACCESS.2020.3047351.

Jung, S. and Dorf, R. C. (1996a). Novel Analytic Technique for PID and PIDA Controller Design. *IFAC Proceedings Volumes*, 29, pp. 1146–1151. *13th World Congress of IFAC, 1996, San Francisco USA, 30 June–5 July*. doi: 10.1016/S1474-6670(17)57819-2.

Jung, S. and Dorf, R. C. (1996b). Analytic PIDA controller design technique for a third order system. In: *Proceedings of the 35th IEEE Conference on Decision and Control*, Vol. 3, pp. 2513–2518 vol. 3.

Khalil, H. (1996). *Nonlinear Systems*, 2nd ed. London: Prentice Hall.

Kothare, M. V., Campo, P. J., Morari, M. and Nett, C. V. (1994). A Unified Framework for the Study of

Anti-windup Designs. *Automatica*, 30, pp. 1869–1883. doi: 10.1016/0005-1098(94)90048-5.

Kumar, M., Hote, Y. V. and Sikander, A. (2023). A novel cascaded CDM-IMC based PIDA controller design and its application. In: *Proceedings of the 2023 IEEE IAS Global Conference on Renewable Energy and Hydrogen Technologies (GlobConHT)*, 11–12 March 2023, Male, Maldives: IEEE, pp. 1–7. doi: 10.1109/GlobConHT56829.2023.10087714.

Kumar, M. and Hote, Y. V. (2021a). Robust PIDD2 Controller Design for Perturbed Load Frequency Control of an Interconnected Time-Delayed Power Systems. *IEEE Transactions on Control Systems Technology*, 29, pp. 2662–2669. doi: 10.1109/TCST.2020.3043447.

Kumar, M. and Hote, Y. V. (2021b). Real-Time Performance Analysis of PIDD2 Controller for Nonlinear Twin Rotor TITO Aerodynamical System. *Journal of Intelligent and Robotic Systems: Theory and Applications*, 101. doi: 10.1007/s10846-021-01322-4.

Kumar, M. and Hote, Y. V. (2021c). PIDD2 controller design based on internal model control approach for a non-ideal DC-DC boost converter. In: *Proceedings of the 2021 IEEE Texas Power and Energy Conference (TPEC)*, 02–05 February 2021, College Station, TX, USA: IEEE. doi: 10.1109/TPEC51183.2021.9384954.

Lima, T. A. (2021). Contributions to the Control of Input-Saturated Systems: Time Delay and allocation Function Cases. Fortaleza: Universidade Federal Do Ceara.

Micev, M., Ćalasan, M. and Radulović, M. (2021). Optimal design of real PID plus second-order derivative controller for AVR system. In: *Proceedings of the 2021 25th International Conference on Information Technology (IT)*, 16–20 February 2021, Zabljak, Montenegro: IEEE, pp. 1–4. doi: 10.1109/IT51528.2021.9390145.

Oladipo, S., Sun, Y. and Wang, Z. (2021). An effective hFPAPFA for a PIDA-based hybrid loop of Load Frequency and terminal voltage regulation system. In *Proceedings of the 2021 IEEE PES/IAS PowerAfrica*, 23–27 August 2021, Nairobi, Kenya: IEEE, pp. 1–5. doi: 10.1109/PowerAfrica52236.2021.9543348.

Oldenbourg, R. and Sartorius, H. (1944). *Dynamik selbsttatiger Regelungen*. Munchen: R.Oldenbourg-Verlag.

Popov, V. (1961). On the Absolute Stability of Nonlinear Control Systems. *Avtom. i telemekhanika*, 22(8), pp. 961–979.

Sahib, M. A. (2015). A Novel Optimal PID Plus Second Order Derivative Controller for AVR System. *Engineering Science and Technology, an International Journal*, 18, pp. 194–206. doi: 10.1016/j.jestch.2014.11.006.

Saxena, S. and Biradar, S. (2022). Fractional-order IMC Controller for High-Order System using Reduced-Order Modelling via Big-Bang, Big-Crunch Optimisation. *International Journal of Systems Science*, 53, pp. 168–181. doi: 10.1080/00207721.2021.1942587.

Takahashi, Y., Chan, C. and Auslander, D. (1971). Parametereinstellung bei linearen DDC-Algorithmen. *Regelungstechnik*, 19, pp. 237–244.

Tepljakov, A., Alagoz, B. B., Yeroglu, C., Gonzalez, E., HosseinNia, S. H. and Petlenkov, E. (2018). FOPID Controllers and Their Industrial Applications: A Survey of Recent Results. *IFAC-PapersOnLine*, 51, pp. 25–30. *3rd IFAC Conference on Advances in Proportional-Integral-Derivative Control PID 2018*. doi: 10.1016/j.ifacol.2018.06.014.

Thomson, D. and Padula, F. (2022). Introduction to Fractional-Order Control: A Practical Laboratory Approach. *IFAC-PapersOnLine*, 55, pp. 126–131. *13th IFAC Symposium on Advances in Control Education ACE 2022*. doi: 10.1016/j.ifacol.2022.09.268.

Ukakimaparn, P., Pannil, P., Boonchuay, P. and Trisuwannawat, T. (2009). PIDA controller designed by Kitti's method. In *Proceedings of the 2009 ICCAS-SICE*, 18–21 August 2009, Fukuoka, Japan: IEEE, pp. 1547–1550.

Veinovic, S., Stojic, D. and Ivanovic, L. (2023). Optimized PIDD2 Controller for AVR Systems Regarding Robustness. *International Journal of Electrical Power and Energy Systems*, 145, p. 108646. doi: 10.1016/j.ijepes.2022.108646.

Visioli, A. and Sánchez-Moreno, J. (2022). A Relay-Feedback Automatic Tuning Methodology of PIDA Controllers for High-Order Processes. *International Journal of Control*, 0, pp. 1–8.

Viteckova, M. and Vitecek, A. (2016). 2DOF PID controller tuning for integrating plants. In: *2016 17th International Carpathian Control Conference (ICCC)*, 29 May 2016–01 June 2016, High Tatras, Slovakia: IEEE, pp. 793–797. doi: 10.1109/CarpathianCC.2016.7501204.

Zandavi, S. M., Chung, V. and Anaissi, A. (2022). Accelerated Control Using Stochastic Dual Simplex Algorithm and Genetic Filter for Drone Application. *IEEE Transactions on Aerospace and Electronic Systems*, 58, pp. 2180–2191. doi: 10.1109/TAES.2021.3134751.

Ziegler, J. G. and Nichols, N. B. (1942). Optimum Settings for Automatic Controllers. *Transactions of the ASME*, 64, pp. 759–768.